

TEMPERATURE AND ELECTRIC POTENTIAL DISTRIBUTION IN THE STRUCTURE PYROELECTRIC-LIQUID CRYSTAL UNDER THE ACTION OF LASER RADIATION

V. N. Shut, A. V. Gavrilov,
and V. L. Trublovskii

UDC 621.319.1

The temperature and electric potential distribution in the structure pyroelectric-liquid crystal under the action of laser radiation has been investigated by numerical methods. The influence of the layer characteristics and modulation frequency of the heat flow on the pyrosignal and its thermal "diffusion" has been considered.

Keywords: IR detector, pyroelectric constant, liquid crystals.

Introduction. To detect radiation, various sensors whose characteristics change under the action of certain wavelengths are used. Thermal radiation can be converted to electric signals by the quantum of thermal sensors. Quantum sensors are based on semiconductors of the type of cadmium mercury telluride ($\text{Cd}_x\text{Hg}_{1-x}\text{Te}$) or indium antimonide (InSb), as well as on metal-semiconductor structures (Schottky diodes) [1, 2]. However, these materials require deep cooling for their operation and are effective only in the visible and near IR region of the spectrum. The range of wavelengths close to $10\ \mu\text{m}$ is of particular interest since it is precisely in this region that the radiation of room-temperature objects reaches the maximum intensity. Therefore, for the given spectral range, thermal sensors based on pyroelectric materials [3] are used successfully for both temperature measurements and thermal-to-visible image conversion. Observation of infrared images is widely practiced in medical diagnostics, nondestructive testing, etc. Of particular interest is the creation of simple and reliable devices for diagnosing mode structures of IR lasers. For visualization of thermal objects, much consideration has been given to the development of pyroelectric matrices, which is due to their compatibility with silicon charge-coupled devices (CCD) [4]. However, making such devices is a complicated technological problem [5].

Pyroelectric materials convert thermal radiation to the spatial distribution of coupled charges on their surface. Therefore, it is possible to convert infrared images directly to visible ones if pyroelectric materials (PE) are combined with an adequate electro-optic medium. For the latter, liquid crystals (LC) [6] can be used. This fact is largely determined by the unique properties of liquid crystals, namely their high sensitivity to control actions, high steepness of the modulation characteristic, and ease of manufacture of multielement instruments and large-format devices on their basis [7]. The present paper gives the results of theoretical investigations of the characteristics of an image converter based on PE-LC structures under the action of laser radiation.

Theoretical Model. The image converter represents a two-dimensional layer structure: pyroelectric-LC-glass substrate (Fig. 1). The thermal energy absorbed by the pyroelectric is converted to an electric signal. In the case of sufficiently powerful radiation, e.g., laser radiation, the electric signal may turn out to be strong enough to change the optical properties of the LC layer. The pyroelectric-LC-substrate structure can be described by means of an equivalent circuit (Fig. 2) — a current generator loaded with parallel-connected capacitors and pyroelectric resistors and LC [8].

A change in the average temperature of the pyroelectric bulk dSd_{PE} by the value ΔT in the crystal leads to a change in the spontaneous polarization P_s by the value

$$\Delta P_s = \gamma \Delta T. \quad (1)$$

In so doing, the charge dq evolved on a polarized surface of area dS is defined by the expression

Institute of Applied Acoustics, National Academy of Sciences of Belarus, 13 Lyudnikov Ave., Vitebsk, 210023, Belarus; email: shut@vitebsk.by. Translated from *Inzhenerno-Fizicheskii Zhurnal*, Vol. 82, No. 4, pp. 721–725, July–August, 2009. Original article submitted April 17, 2008; revision submitted September 26, 2008.

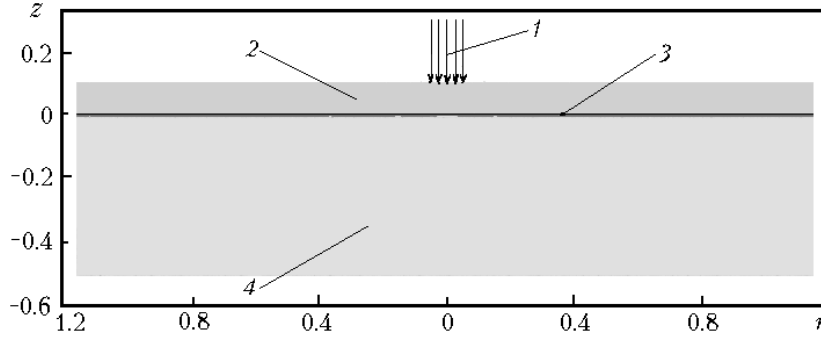


Fig. 1. Schematic representation of the structure of the image converter: 1) laser beam; 2) pyroelectric; 3) LC layer; 4) substrate.

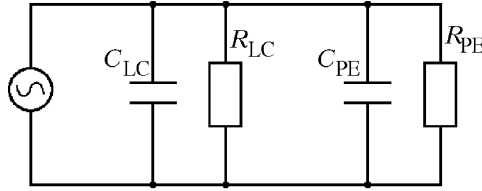


Fig. 2. Equivalent circuit of the pyroelectric-liquid crystal structure.

$$dq = dS \Delta P_s. \quad (2)$$

If the change in the thickness-average temperature of the pyroelectric obeys the sinusoidal law with angular oscillation frequency $\omega = 2\pi f$ and amplitude T_m , then current $dI = \gamma dS \frac{dT}{dt}$ with oscillation frequency

$$I_m = \gamma dS \omega T_m \quad (3)$$

will flow through dS .

The load impedance modulus (of the pyroelectric and LC) with area dS is defined by the following expression:

$$|Z| = \frac{R}{\sqrt{1 + \omega^2 R^2 C^2}} \approx \frac{R_{LC}}{\sqrt{1 + \omega^2 R_{LC}^2 C^2}}, \quad (4)$$

since $R_{PE} \gg R_{LC}$ for pyroelectric layer thicknesses larger than $10 \mu\text{m}$.

Taking into account that $R_{LC} = \rho_{LC} d_{LC} / dS$, $C = C_{LC} + C_{PE} = \epsilon_0 dS (\epsilon_{LC} / d_{LC} + \epsilon_{PE} / d_{PE})$, we represent expression (4) in the form

$$|Z| = \frac{1}{dS} \frac{\rho_{LC} d_{LC}}{\sqrt{1 + \omega^2 (\epsilon_0 \rho_{LC} d_{LC} (\epsilon_{LC} / d_{LC} + \epsilon_{PE} / d_{PE}))^2}}. \quad (5)$$

Thus, with the use of expressions (3) and (5) we can find the value of the amplitude of voltage oscillations between the surfaces of the pyroelectric plate at any point ($dS \rightarrow 0$)

$$U_m = |Z| I_m = \gamma \omega T_m \frac{\rho_{LC} d_{LC}}{\sqrt{1 + \omega^2 (\epsilon_0 \rho_{LC} d_{LC} (\epsilon_{LC} / d_{LC} + \epsilon_{PE} / d_{PE}))^2}}. \quad (6)$$

Knowing the temperature distribution in the pyroelectric target, it is fairly easy to find the value of U_m . The temperature distribution in the pyroelectric target can be described by the heat conduction equation

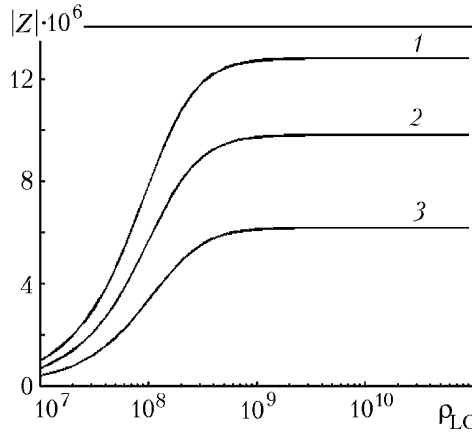


Fig. 3. Total resistance modulus $|Z|$ of the pyroelectric–liquid crystal structure of area 1 cm^2 versus the specific resistance of the LC layer ρ_{LC} at $f = 10 \text{ Hz}$, $d_{PE} = 100 \text{ }\mu\text{m}$: 1) $d_{LC} = 10 \text{ }\mu\text{m}$; 2) 7; 3) 4. Z, Ω ; $\rho_{LC}, \Omega\cdot\text{m}$.

TABLE 1. Distance from the Laser Beam Center at Which the Pyrosignal Amplitude U_m Is Smaller than the Maximum Value (in the center $r = 0$) by a Factor of $e \approx 2.72$

$f, \text{ Hz}$	$d_{PE}, \mu\text{m}$				
	10	25	50	100	200
10	75	87	97	104	109
30	69	77	81	84	87
100	62	65	66	67	68

$$c\rho^* \frac{\partial T}{\partial t} - k\Delta T = 0 \quad (7)$$

with boundary conditions of the 3d kind:

a) for the surface subjected to laser radiation with heat flow density W

$$\mathbf{n} k \text{ grad } T = \sigma (T_0 - T) + W, \quad (8)$$

b) for the rest of the surface

$$\mathbf{n} k \text{ grad } T = \sigma (T_0 - T). \quad (9)$$

In the case of axial symmetry, to which the problem under consideration corresponds, Eqs. (7)–(9) in the cylindrical system of coordinates will take on the following form: of the heat conduction equation

$$c\rho^* \frac{\partial T}{\partial t} - k \left(\frac{1}{r} \frac{\partial}{\partial r} \left(r \frac{\partial T}{\partial r} \right) + \frac{\partial^2 T}{\partial z^2} \right) = 0 \quad (10)$$

with boundary conditions of the 3d kind:

a) for the surface subjected to the laser radiation

$$k \frac{\partial T}{\partial z} = \sigma (T - T_0) + W, \quad (11)$$

b) for the rest of the surface of the target bases

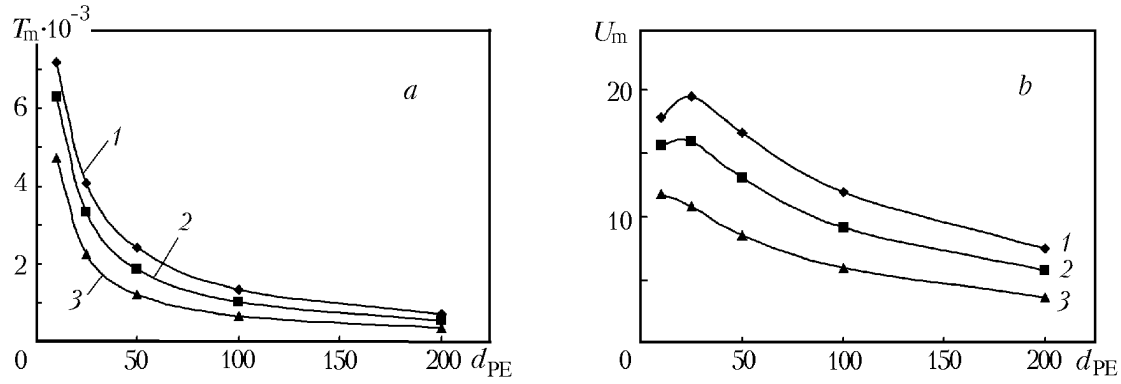


Fig. 4. Temperature oscillation amplitude of the pyroelectric plate (thickness-average value) T_m (a) and voltage amplitude U_m on the LC layer (b) in the center of the laser beam (of radius $50 \mu\text{m}$, $W = 100 \text{ W/m}^2$) versus the pyroelectric thickness d_{PE} for radiation modulation frequencies: 1) $f = 10 \text{ Hz}$; 2) 30; 3) 100. T_m , $^{\circ}\text{C}$; U_m , mV; d_{PE} , μm .

$$k \frac{\partial T}{\partial z} = \sigma (T - T_0), \quad (12)$$

c) for the lateral surface of the target

$$k \frac{\partial T}{\partial r} = \sigma (T - T_0). \quad (13)$$

As a pyroelectric layer of the target, we considered lithium tantalate (LiTaO_3) monocrystals (plates of thickness $d_{PE} = 25\text{--}300 \mu\text{m}$, heat conduction $k = 3 \text{ W/(m}\cdot\text{K)}$, heat capacity $c = 430 \text{ J/(kg}\cdot\text{K)}$, density $\rho_{PE} = 7400 \text{ kg/m}^3$). It was assumed that a laser beam having a circular cross-section of diameter $100 \mu\text{m}$ was incident perpendicularly to the plate (Fig. 1), and the heat flow density W_m thereby was time-independent and invariable within the cross-section of the beam. The laser-generated heat flow was chopped by a chopper with a frequency of $f = 10\text{--}100 \text{ Hz}$ by the sinusoidal law

$$W = W_m \left(\frac{\sin(\omega t) + 1}{2} \right). \quad (14)$$

Results and Discussion. Analysis of Eqs. (5) and (6) has shown that the amplitude of the pyrosignal U_m is determined by both the value of the temperature oscillation amplitude in the pyroelectric plate T_m and the value of the total resistance $|Z|$ of the pyroelectric–liquid crystal structure. The value of $|Z|$ increases monotonically with increasing specific resistance of the LC layer up to $10^9 \Omega\cdot\text{m}$ (Fig. 3). The thicknesses of LC cells were chosen proceeding from the possibilities of modern technologies: $4\text{--}10 \mu\text{m}$. A further increase in the resistance of the LC layer does not lead to a change in the total resistance of the pyroelectric–liquid crystal structure. This is due to the fact that the quantity $(\omega RC)^2$ in expression (4) takes on values greater than unity.

The voltage created in the electrooptical layer depends also on the pyroelectric thickness and the modulation frequency. With decreasing thickness d_{PE} of the pyroelectric layer the maximum temperature oscillations T_m in the region of the laser beam spot increase (Fig. 4a). On the other hand, there is an increase in the pyroelectric capacity, which leads to a decrease in the load resistance (expression (5)). Therefore, maximum values of the signal on the LC are observed when the pyroelectric thickness is of the order of a few tens of microns (Fig. 4b). The pyrosignal value increases with decreasing modulation frequency.

In the case of matrix pyroelectric targets, individual pixels, as a rule, are heat-insulated from one another. In our case, such heat-insulation is absent. This leads to the fact that under external action the temperature changes not only in the portions on which the radiation is incident but also in adjacent regions, i.e., "thermal diffusion" of the image takes place, which leads to a decrease in the resolution of the device. Image diffusion is determined by both

the pyroelectric target thickness and the radiation modulation frequency. The table gives the distance from the center of the laser beam at which the pyrosignal amplitude decreases by a factor of $e \approx 2.72$. It is seen that this distance decreases with increasing modulation frequency and decreasing pyroelectric thickness. In so doing, the spatial resolution of the structure depends on the modulation frequency to a lesser extent when thinner pyroelectric targets are used.

Conclusions. Investigations of the temperature and voltage distribution between the pyroelectric plate surfaces in the pyroelectric–LC structure under the action of laser radiation have been carried out. It has been established that for attaining the maximum value of the pyrosignal, pyroelectric layer thicknesses of $\sim 20 \mu\text{m}$ and specific resistance values of the LC layer higher than $10^9 \Omega\cdot\text{m}$ are optimal. It has been shown that the converter resolution increases with increasing modulation frequency of the thermal radiation and decreasing thickness of the pyroelectric. The investigated structures may be of interest for visualizing mode structures of IR lasers.

NOTATION

C , capacitance, F; c , specific heat capacity, J/(kg·K); d , thickness, μm ; f , frequency, Hz; I , current, A; k , heat conductivity, W/(m·K); \mathbf{n} , unit normal vector to the surface; P_s , spontaneous polarization, C/m²; q , charge, C; R , resistance, Ω ; r , coordinate, mm; S , area, m²; T , temperature, °C; t , time, sec; U , voltage, mW; W , heat flow density, W/m²; Z , resistance (complex impedance), Ω ; z , coordinate, mm; γ , pyroelectric coefficient, C/(m²·K); ϵ_0 , electric constant, F/m; ϵ , relative permittivity; ρ , specific resistance, $\Omega\cdot\text{m}$; ρ^* , density, kg/m³; σ , heat transfer coefficient of the surface, W/(m²·K); ω , angular frequency, Hz. Subscripts: 0, environment; m, maximum amplitude value; s, spontaneous; LC, LC layer; PE pyroelectric layer.

REFERENCES

1. W. F. Kosonocky, Visible and infrared solid-state image sensors, *Int. Electron Devices Meeting*, **29**, 1–7 (1983).
2. M. Denda, M. Kimata, N. Yutani, N. Tsubouchi, and S. Uematsu, A PtSi Schottky-barrier infrared MOS area imager with large fill factor, *Int. Electron Devices Meeting*, **29**, 722–725 (1983).
3. S. B. Lang, Review of recent work on pyroelectric applications, *Ferroelectrics*, **53**, 189–196 (1984).
4. R. Watton, P. Manning, D. Burgess, and J. Gooding, The pyroelectric/CCD focal plane hybrid: Analysis and design for direct charge injection, *Infrared Phys.*, **22**, 259–275 (1982).
5. P. Murali, Micromachined infrared detectors based on pyroelectric thin films, *Rep. Prog. Phys.*, **64**, 1339–1342 (2001).
6. L. Turi, P. Kalman, and A. Toth, Pyrooptic converter, a new device for wavelength conversion of electromagnetic radiation, *Ferroelectrics*, **99**, 239–245 (1989).
7. E. Lueder, *Liquid Crystal Displays*, Wiley Series, New York (2001).
8. V. F. Kosorotov, L. S. Kremenchugskii, V. B. Samoilov, and L. V. Shchedrina, *Pyroelectric Effect and Its Practical Applications* [in Russian], Naukova Dumka, Kiev (1989).